# Refined finite element of rods for stability calculation

# Улучшенный стержневой конечный элемент для решения задач устойчивости

**Yu.Ya. Tyukalov,**
*Vyatka State University, Kirov, Russia*

**Д-р техн. наук, профессор Ю.Я. Тюкалов,**
*Вятский государственный университет, Киров, Россия*

**Abstract.** The article deals with the application of a rod finite element with five degrees of freedom in a node to solve problems of stability of planar rod systems. In the presented finite element, additional degrees of freedom are introduced in the nodes in the form of curvature and axial deformation. Additional degrees of freedom provide a higher degree of approximation of displacements and deformations along the length of the finite element, which can be useful for calculation of rods with variable rigidity, as well as for solving geometrically nonlinear problems and stability problems. In this paper the elements of stiffness matrix and the elements of geometric matrix of the finite element are obtained. The results of the calculation of straight rods and frames under various conditions of support and various loads are presented. A comparison is made with the results of calculations using a classic finite element with three degrees of freedom. It is shown that the introduction of additional degrees of freedom at the nodes, in the form of the curvature of the axis and longitudinal deformation, makes it possible in a few cases to more accurately determine the value of the critical load. In this case, the system has more degrees of freedom, so the approximation of the forms of stability loss is more accurate.

**Аннотация.** В статье рассматривается применение стержневого конечного элемента с пятью степенями свободы в узле для решения задач устойчивости плоских стержневых систем. В представленном конечном элементе в узлах введены дополнительные степени свободы в виде кривизны и осевой деформации. Дополнительные степени свободы обеспечивают более высокую степень аппроксимации перемещений и деформаций по длине конечного элемента, что может быть полезным для стержней переменной жесткости, а также при решении геометрически нелинейных задач и задач устойчивости. В работе получены элементы матрицы жесткости и геометрической матрицы конечного элемента. Представлены результаты расчетов прямых стержней и рам при различных условиях вариантах опор и нагрузок. Выполнено сравнение с результатами расчетов при использовании конечного элемента с тремя степенями свободы. Показано, что ведение дополнительных степеней свободы в узлах, в виде кривизны оси и продольной деформации, позволяет в ряде случаев более точно определить величину критической нагрузки. В этом случае система имеет больше степеней свободы, поэтому аппроксимация форм потери устойчивости является более точной.

## 1. Introduction

Numerous fundamental studies, including papers [1–3], have been devoted to the calculation of various constructions by the finite element method. For rod systems, most attention is paid to the construction of functionals for solving stability problems of rods [4], as well as to the methods calculations constructions considering geometric and physical nonlinearities [5, 6]. In paper [7], an exact, analytical solution of the beam bending problem is constructed according to Euler-Bernoulli and Timoshenko theories. The work [8] is devoted to the determination of critical forces by the flexural-torsional form of the loss of stability of steel columns with allowance for physical nonlinearity. In [9, 10] we consider the computational efficiency of the proposed method of quadrature finite elements for calculating the stability of planar rod systems. In these articles the rods of constant and variable cross sections are considered and comparison of the proposed method of calculation with the finite element method in displacements is performed.

To analyze the stability of rods, models based on plane stress finite elements can be used. In [11] the steel I-beam is modeled by such plane finite elements and the influence of the compressive load

distribution law over cross section to the critical value of the load is studied. In [12, 13] we consider the calculation of the stability of perforated steel columns. In [12] the calculation of stability of perforated columns is based on the approximation of transverse and longitudinal displacements by trigonometric functions and the obtained solutions compares with the solutions by the finite element method.

In article [14] the influence of the position of the compressive load in the calculation of the stability of flat steel frames is studied. The load in the form of a concentrated force applied to the beam is considered and the influence of its position on the value of the critical load is determined. The solution is constructed by the finite element method.

The paper [15] presents numerical studies of possible scenarios for the loss of stability of flat arches using the NASTRAN program. Many papers are devoted to the calculation of thin-walled rod systems by the finite element method [16, 17] and to the study of various variational formulations of stability problems of planar systems and geometrically nonlinear deformation of rod systems [18–19]. Features of the calculation of the stability of bars in the exact formulation are considered in [20–22]. In this case, the solution reduces to a system of transcendental equations. This approach is highly accurate but can only be used for simple systems.

In [23, 24] the solutions of stability problems and free vibrations of rod systems are based on the functional of additional energy and the using approximations for the forces. It is shown that with this approach one can obtain the upper limits of the critical forces and of the frequencies of free oscillations.

In [25] a finite element with five degrees of freedom in a node is used to calculating planar rod systems with allowance for physical nonlinearity. Additional degrees of freedom provide better approximation of displacements and deformations along the length of the finite element, what can be useful for calculating the rods of variable rigidity, as well as for solving geometrically nonlinear problems and stability problems. Note, that in solving static problems of rods bending by the finite element method, a cubic polynomial function is used to approximate transverse displacements, which ensures the obtaining of exact values of internal forces. But under the action of distributed loads, the displacements along the length of the beam vary according to the polynomial of the fifth degree and so a cubic polynomial function can't provide the exact values of the displacements.

The aim of this paper is to construct a more accurate solution to the problem of stability of planar rod systems using the finite element with five degrees of freedom at nodes. The main tasks are: obtaining expressions for the elements of the stiffness matrix and the geometric matrix of the rod finite element with five degrees of freedom in the node; the development of an algorithm for calculating the stability of planar rod systems; comparison of the results of the determination of critical parameters for various rod systems, according to the proposed methodology, with the results obtained using the LIRA-SAPR program, which uses a finite element with three degrees of freedom.

## *2. Methods*

In paper [23] the rod finite element with five degrees of freedom at a node (Figure 1) is used to solve the dynamic problems of reinforced concrete planar bar systems with allowance for physical nonlinearity. In this finite element additional degrees of freedom were introduced in the form of curvature and axial deformation. Note that the curvatures and axial deformations in the node are different for the finite elements adjacent to this node. Therefore, the total number of unknowns for the whole system is $n = 3k_n + 4k_e - s$. $k_n$ – number of nodes; $k_e$ – number of finite elements; $s$ – the number of superimposed links. On the other hand, such the finite element provides an accurate calculation of deformations and stresses and ensures, if necessary, their continuity. As is known, when using a standard rod finite element, with three degrees of freedom, gaps of deformations and stresses may appear at the nodes, for example, at the start or end points of a distributed load. In addition, direct calculation of deformations and ensuring continuity of stresses makes it easier to obtain of solving physically nonlinear problem and can improve the accuracy of calculations. Also, when solving stability problems, increasing the number of degrees of freedom makes the system more flexible and, therefore, leads to smaller and more accurate values of the critical forces.

We use this finite element to solve the problem of determining the critical load for planar rod systems. At the first stage, it is necessary to determine the internal forces (longitudinal forces) in the rods from the action of the applied loads. In Figure 1 this finite element is represented and the following notations are introduced: $w_1, w_2$ – displacements of nodes along the $Y_1$ axis; $\varphi_1, \varphi_2$ – angles of rotation of sections; $u_1, u_2$ – displacements of nodes along the $X_1$ axis; $k_1, k_2$ – the curvatures of the axes at the nodes; $\varepsilon_1, \varepsilon_2$ – axial deformations at the nodes.
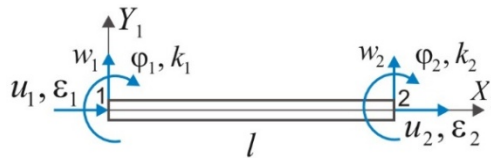
**Figure 1. Finite element with five degrees of freedom in the node**

The transverse displacement of the axis of the finite element is represented by the polynomial of the fifth degree in the following form:

$$w(x) = L_1(x)w_1 + L_2(x)\varphi_1 + L_3(x)k_1 + L_4(x)w_2 + L_5(x)\varphi_2 + L_6(x)k_2, \tag{1}$$

where:

$$L_1(x) = 1 - 10\left(\frac{x}{l}\right)^3 + 15\left(\frac{x}{l}\right)^4 - 6\left(\frac{x}{l}\right)^5,$$

$$L_2(x) = l\left[\frac{x}{l} - 6\left(\frac{x}{l}\right)^3 + 8\left(\frac{x}{l}\right)^4 - 3\left(\frac{x}{l}\right)^5\right],$$

$$L_3(x) = \frac{l^2}{2}\left[\left(\frac{x}{l}\right)^2 - 3\left(\frac{x}{l}\right)^3 + 3\left(\frac{x}{l}\right)^4 - \left(\frac{x}{l}\right)^5\right],$$

$$L_4(x) = 10\left(\frac{x}{l}\right)^3 - 15\left(\frac{x}{l}\right)^4 + 6\left(\frac{x}{l}\right)^5, \tag{2}$$

$$L_5(x) = l\left[-4\left(\frac{x}{l}\right)^3 + 7\left(\frac{x}{l}\right)^4 - 3\left(\frac{x}{l}\right)^5\right],$$

$$L_6(x) = \frac{l^2}{2}\left[\left(\frac{x}{l}\right)^3 - 2\left(\frac{x}{l}\right)^4 + \left(\frac{x}{l}\right)^5\right].$$

Longitudinal displacements are approximated by the polynomial of the third degree:

$$u(x) = L_7(x)u_1 + L_8(x)\varepsilon_1 + L_9(x)u_2 + L_4(x)\varepsilon_2, \tag{3}$$

$$L_7(x) = 1 - 3\left(\frac{x}{l}\right)^2 + 2\left(\frac{x}{l}\right)^3,$$

$$L_8(x) = l\left[\frac{x}{l} - 2\left(\frac{x}{l}\right)^2 + \left(\frac{x}{l}\right)^3\right],$$

$$L_9(x) = 3\left(\frac{x}{l}\right)^2 - 2\left(\frac{x}{l}\right)^3, \tag{4}$$

$$L_8(x) = l\left[-\left(\frac{x}{l}\right)^2 + \left(\frac{x}{l}\right)^3\right].$$

The unknowns and the form functions are combined into vectors:

$$\{w_e\} = \begin{Bmatrix} w_1 \\ \varphi_1 \\ k_1 \\ w_2 \\ \varphi_2 \\ k_2 \end{Bmatrix}, \qquad \{L_w\} = \begin{Bmatrix} L_1(x) \\ L_2(x) \\ L_3(x) \\ L_4(x) \\ L_5(x) \\ L_6(x) \end{Bmatrix}, \qquad \{u_e\} = \begin{Bmatrix} u_1 \\ \varepsilon_1 \\ u_2 \\ \varepsilon_2 \end{Bmatrix}, \qquad \{L_u\} = \begin{Bmatrix} L_7(x) \\ L_8(x) \\ L_9(x) \\ L_{10}(x) \end{Bmatrix}. \tag{5}$$

When solving problems of stability, without considering the shear strains, deformations are expressed in the following form [1]:

$$\varepsilon_x = \frac{du}{dx} - z\frac{d^2w}{dx^2} + \frac{1}{2}\left(\frac{dw}{dx}\right)^2. \tag{6}$$

Then the strain energy of the finite element is expressed in the following form [1, 2]:

$$U^e = \frac{1}{2}\int_0^l \left[EI\left(\frac{d^2w}{dx^2}\right)^2 + EA\left(\frac{du}{dx}\right)^2 + N(x)\left(\frac{dw}{dx}\right)^2\right]dx. \tag{7}$$

where: $EI$, $EA$ – flexural and longitudinal stiffness of cross-section of the element. The longitudinal force can vary along the length of the finite element, so we assume that

$$N(x) = N_1(1 - x/l) + N_2\, x/l, \tag{8}$$

where: $N_1, N_2$ – longitudinal forces at the beginning and end of the finite element.

Using (1 5), we write expression (7) in the matrix form:

$$U^e = \frac{1}{2}(\{w_e\}^T[k_w]\{w_e\} + \{u_e\}^T[k_u]\{u_e\} + \{w_e\}^T[k_N]\{w_e\}), \tag{9}$$

$$[k_w] = \int_0^l EI\{L_w''\}\{L_w''\}^T dx, \; [k_u] = \int_0^l EA\{L_u'\}\{L_u'\}^T dx, \; [k_N] = \int_0^l N(x)\{L_w'\}\{L_w'\}^T dx. \tag{10}$$

We unite the nodal unknowns into one vector

$$\{y_e\} = \begin{Bmatrix} \{w_e\} \\ \{u_e\} \end{Bmatrix}. \tag{11}$$

The expression (8) can be written in the following form:

$$U^e = \frac{1}{2}\{y_e\}^T([k_e] + [k_{Ne}])\{y_e\}, \tag{12}$$

$$[k_e] = \begin{bmatrix}
\frac{120\cdot EI}{7\cdot l^3} & \frac{60\cdot EI}{7\cdot l^2} & \frac{3\cdot EI}{7\cdot l} & \frac{-120\cdot EI}{7\cdot l^3} & \frac{60\cdot EI}{7\cdot l^2} & \frac{-3\cdot EI}{7\cdot l} & 0 & 0 & 0 & 0 \\
 & \frac{192\cdot EI}{35\cdot l} & \frac{11\cdot EI}{35} & \frac{-60\cdot EI}{7\cdot l^2} & \frac{108\cdot EI}{35\cdot l} & \frac{-4\cdot EI}{35} & 0 & 0 & 0 & 0 \\
 & & \frac{3\cdot l\cdot EI}{35} & \frac{-3\cdot EI}{7\cdot l} & \frac{4\cdot EI}{35} & \frac{EI\cdot l}{70} & 0 & 0 & 0 & 0 \\
 & & & \frac{120\cdot EI}{7\cdot l^3} & \frac{-60\cdot EI}{7\cdot l^2} & \frac{3\cdot EI}{7\cdot l} & 0 & 0 & 0 & 0 \\
 & & & & \frac{192\cdot EI}{35\cdot l} & \frac{-11\cdot EI}{35} & 0 & 0 & 0 & 0 \\
 & & & & & \frac{3\cdot l\cdot EI}{35} & 0 & 0 & 0 & 0 \\
 & & & & & & \frac{6\cdot EA}{5\cdot l} & \frac{EA}{10} & \frac{-6\cdot EA}{5\cdot l} & \frac{EA}{10} \\
 & & & & & & & \frac{2\cdot l\cdot EA}{15} & \frac{-EA}{10} & \frac{-l\cdot EA}{30} \\
 & & & & & & & & \frac{6\cdot EA}{5\cdot l} & \frac{-EA}{10} \\
 & & & & & & & & & \frac{2\cdot l\cdot EA}{15}
\end{bmatrix}, \tag{13}$$

$$[k_{Ne}] = \begin{bmatrix}
\frac{5(N_1+N_2)}{7\cdot l} & \frac{5N_1+13N_2}{84} & \frac{N_2 l}{84} & \frac{-5(N_1+N_2)}{7\cdot l} & \frac{13N_1+5N_2}{84} & \frac{-N_1 l}{84} & 0 & 0 & 0 & 0 \\
 & \frac{N_1 l}{6}+\frac{13N_2 l}{210} & \frac{11N_1 l^2}{1008}+\frac{29N_2 l^2}{5040} & \frac{-5N_1-13N_2}{84} & \frac{-(N_1+N_2)l}{140} & \frac{(11N_1+13N_2)l^2}{5040} & 0 & 0 & 0 & 0 \\
 & & \frac{N_1 l^3}{1008}+\frac{N_2 l^3}{1680} & \frac{-N_2 l}{84} & \frac{-(13N_1+11N_2)l^2}{5040} & \frac{(N_1+N_2)l^3}{2520} & 0 & 0 & 0 & 0 \\
 & & & \frac{5(N_1+N_2)}{7\cdot l} & \frac{-13N_1-5N_2}{84} & \frac{N_1 l}{84} & 0 & 0 & 0 & 0 \\
 & & & & \frac{13N_1}{210}+\frac{N_2 l}{6} & \frac{-29N_1 l^2}{5040}-\frac{11N_2 l^2}{1008} & 0 & 0 & 0 & 0 \\
 & & & & & \frac{N_1 l^3}{1680}+\frac{N_2 l^3}{1008} & 0 & 0 & 0 & 0 \\
 & & & & & & 0 & 0 & 0 & 0 \\
 & & & & & & & 0 & 0 & 0 \\
 & & & & & & & & 0 & 0 \\
 & & & & & & & & & 0
\end{bmatrix}. \tag{14}$$

The matrices (13) and (14) are symmetric, therefore the matrix elements above the main diagonal are shown.
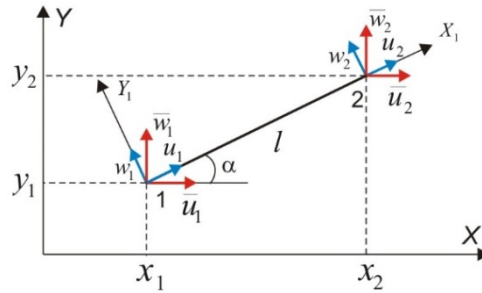
**Figure 2. Global and local coordinate systems.**

In Figure 2 shows the global and local coordinate systems. Nodal unknowns in the global coordinate system are indicated by an upper line. Vectors of nodal unknown finite elements in local $\{y_e\}$ and global coordinate systems $\{\overline{y}_e\}$ are connected by a matrix of directing cosines:

$$\{\overline{y}_e\} = [S]\{y_e\}, \tag{15}$$

$$[S] = \begin{bmatrix} \cos\alpha & 0 & 0 & 0 & 0 & 0 & \sin\alpha & 0 & 0 & 0 \\ 0 & 1 & 0 & 0 & 0 & 0 & 0 & 0 & 0 & 0 \\ 0 & 0 & 1 & 0 & 0 & 0 & 0 & 0 & 0 & 0 \\ 0 & 0 & 0 & \cos\alpha & 0 & 0 & 0 & 0 & \sin\alpha & 0 \\ 0 & 0 & 0 & 0 & 1 & 0 & 0 & 0 & 0 & 0 \\ 0 & 0 & 0 & 0 & 0 & 1 & 0 & 0 & 0 & 0 \\ -\sin\alpha & 0 & 0 & 0 & 0 & 0 & \cos\alpha & 0 & 0 & 0 \\ 0 & 0 & 0 & 0 & 0 & 0 & 0 & 1 & 0 & 0 \\ 0 & 0 & 0 & -\sin\alpha & 0 & 0 & 0 & 0 & \cos\alpha & 0 \\ 0 & 0 & 0 & 0 & 0 & 0 & 0 & 0 & 0 & 1 \end{bmatrix}. \tag{16}$$

Using the vector of nodal unknowns in the global coordinate system, we get:

$$U^e = \frac{1}{2}\{\overline{y}_e\}^T \left([\overline{k}_e] + [\overline{k}_{Ne}]\right)\{\overline{y}_e\}, \tag{17}$$

$$[\overline{k}_e] = [S][k_e][S]^T, \qquad [\overline{k}_{Ne}] = [S][k_{Ne}][S]^T. \tag{18}$$

$[\overline{k}_e]$ is the finite element stiffness matrix in the global coordinate system; $[\overline{k}_{Ne}]$ is the geometric matrix of the finite element in the global coordinate system. From the matrices $[\overline{k}_e]$ and $[\overline{k}_{Ne}]$ of all finite elements of the system, in accordance with the numbering of nodes and elements, the corresponding global matrices – $[K]$ and $[K_N]$ are formed, and the unknowns for the whole system are represented by the vector $\{Y\}$. Then the energy of deformation of all finite elements

$$U = \frac{1}{2}\{Y\}^T \left([K] + [K_N]\right)\{Y\}. \tag{19}$$

To obtain a solution, it is necessary to write down the expression for the potential of external concentrated and distributed forces $V$. For the loads distributed over the length of the finite element, the potential is expressed as the integral

$$V^e = -\int_0^l \left(q_{y_1} w(x) + q_{x_1} u(x)\right) dx, \tag{20}$$

where:

$$q_{y_1} = q_y \cos\alpha - q_x \sin\alpha, \ \ q_{x_1} = q_y \sin\alpha + q_x \cos\alpha. \tag{21}$$

$q_y, q_x$ – values of the loads distributed along the length of the finite element, directed along the global axes Y and X, respectively. For evenly distributed loads:

$$V^e = \{y_e\}^T \{F_e\}, \tag{22}$$

$$\{F_e\}^T = \left(\frac{q_{y_1}L}{2} \quad \frac{q_{y_1}L^2}{10} \quad \frac{q_{y_1}L^3}{120} \quad \frac{q_{y_1}L}{2} \quad \frac{-q_{y_1}L^2}{10} \quad \frac{q_{y_1}L^3}{120} \quad \frac{q_{x_1}L}{2} \quad \frac{q_{x_1}L^2}{12} \quad \frac{q_{x_1}L}{2} \quad \frac{-q_{x_1}L^2}{12}\right). \tag{23}$$

Using the vector of nodal unknowns in the global coordinate system, we get:

$$V^e = \{\overline{y}_e\}^T \{\overline{F}_e\},$$ (24)

$$\{\overline{F}_e\} = [S]\{F_e\}.$$ (25)

From vectors $\{\overline{F}_e\}$ for all finite elements the global vector $\{F\}$ is formed for the whole system. The forces $P_x, P_y$, concentrated in the nodes, which directed along the global axes, and the concentrated in the nodes moments $M$ are added to the corresponding elements of the global vector $\{F\}$.

Using the notation introduced above, we write the total potential energy of the system in the following form:

$$\Pi = U + V = \frac{1}{2}\{Y\}^T([K] + [K_N])\{Y\} + \{Y\}^T\{F\} \rightarrow min.$$ (26)

Equating the derivatives of the total potential energy of the system with along the vector of nodal unknowns to zero, we obtain a system of resolving equations:

$$([K] + [K_N])\{Y\} + \{F\} = 0.$$ (27)

In the classical approach, the matrix $[K_N]$ is not considered when solving the system of equations (27), therefore the values of displacements and internal forces are determined without considering the effect of longitudinal forces on bending. In a more precise variant, the iterative solution of the system (27) is performed and the elements of the matrix $[K_N]$ are calculated using the longitudinal forces obtained in the previous step. For some constructions, solutions for the two options may differ materially.

Solving the system of linear equations (27), we find the displacement vector $\{Y\}_0$ and, further, calculate the longitudinal forces in finite elements. The critical load parameter $\lambda_{cr}$ can be found by the well-known method of reverse iterations. The algorithm consists of the following steps:

$$\begin{cases} i = 1,2, \cdots m; \\ \{Y\}_i = [K]^{-1}[K_N]\{Y\}_{i-1}, \\ y_{max} = \max_{j=1..n}|\{Y\}_i|, \\ \lambda_{cr,i} = \dfrac{1}{|y_{max}|}, \\ \{Y\}_i = \lambda_{cr,i}\{Y\}_i. \end{cases}$$ (28)

In (28) $y_{max}$ is the maximum modulo element of the vector $\{Y\}_i$. The iterative procedure ends when the necessary accuracy is getting for $|\lambda_{cr,i} - \lambda_{cr,i-1}| < \varepsilon$. The vector $\{Y\}_i$ is the vector of the shape of the loss of stability.

## 3. Results and Discussion

As a first example, according to a program compiled in Mathcad 14.0, calculations of the critical forces for straight rods were performed under various conditions of supporting the ends (Figure 3). To simplify the analysis of the results, all the parameters of the rods were equal as single ones. The rod was modeled by only one finite element. Table 1 shows the results of calculations using the proposed finite element and the results of calculations using the LIRA-SAPR program, as well as the exact, analytically obtained values [26].
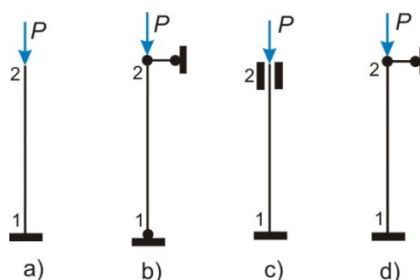


a)   b)   c)   d)

**Figure 3. Variants of support of straight rods.** $l = 1\ m.,\ EI = 1\ kN \cdot m^2$

*Table 1. Critical forces for straight rods (Figure 3)*

| Rod | Finite element with five degrees of freedom | | | Finite element with three degrees of freedom, LIRA-SAPR | | | Exact decision, $P_{cr}, kN$ |
|---|---|---|---|---|---|---|---|
| | $P_{cr}, kN$ | Error, % | Quantity of unknowns | $P_{cr}, kN$ | Error, % | Quantity of unknowns | |
| a) Console rod | 2.4674 | 0 | 7 | 2.486 | 0.75 | 4 | 2.4674 |
| b) Hinged supports | 9.882 | 0.125 | 7 | 12.0 | 21.6 | 3 | 9.8696 |
| c) Clamped ends | 39.480 | 0.004 | 5 | - | - | 1 | 39.4784 |
| d) Clamped and hinged support | 20.347 | 0.77 | 6 | 30 | 48.6 | 2 | 20.1906 |

The obtained solutions show that when using the finite element with five degrees of freedom, the calculated values of the critical forces are very close to the exact values under any conditions of support of the rod ends. The greatest error in the calculation of the critical force of only 0.77 % was obtained for a rod with one pinched and one hinged support end.

When using the classical finite element with three degrees of freedom in a node, for a rod with clamped supports (Figure 3c), a solution can't be obtained, since the calculation scheme with one finite element has only one degree of freedom associated with the longitudinal displacement of the upper node. For this finite element, the exact solution is obtained only for the console rod (Figure 3a), in other cases the errors of the solutions are significant. To obtain more precise solutions, it is obviously necessary to divide the rod into two finite elements, thereby increasing the total number of degrees of freedom.
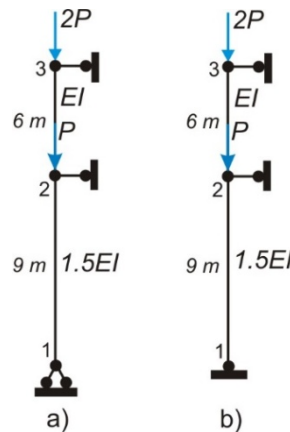


**Figure 4. Straight rods with intermediate support. Flexural stiffness varies stepwise**

In Figure 4 shows straight rods with intermediate supports and with different bending stiffness, varying stepwise. A well-known "forces method" can be used to determine the exact value of the critical load. In this case, the coefficients of the canonical equations are determined based on the exact solution of the differential equation of a compressed-bent rod. We introduce the following notation:

$$\lambda_1 = l_{2-3}\sqrt{\frac{N_{2-3}}{EI}} = 6\sqrt{\frac{2P}{EI}}, \qquad \lambda_2 = l_{1-2}\sqrt{\frac{N_{1-2}}{EI}} = 9\sqrt{\frac{3P}{1.5EI}} = 1.5\lambda_1. \qquad (29)$$

Then the equation of the "forces method" for determining the critical load for the rod in Fig. 4a will be as follows:

$$\frac{3}{\lambda_1}\left(\frac{1}{\lambda_1} - \frac{1}{\tan\lambda_1}\right) + \frac{3}{\lambda_2}\left(\frac{1}{\lambda_2} - \frac{1}{\tan\lambda_2}\right) = \frac{3}{\lambda_1}\left(\frac{1}{\lambda_1} - \frac{1}{\tan\lambda_1}\right) + \frac{2}{\lambda_1}\left(\frac{1}{1.5\lambda_1} - \frac{1}{\tan 1.5\lambda_1}\right) = 0. \quad (30)$$

Тюкалов Ю.Я. Улучшенный стержневой конечный элемент для решения задач устойчивости // Инженерно-строительный журнал. 2018. № 3(79). С. 54–65.

Solving equation (30) in Mathcad 14, we obtain that $\lambda_{1,cr} = 2.355779$. We will take $EI = 1\ kN/m^2$, then $P_{cr} = \frac{1}{2 \cdot 36} \lambda_{1,cr}{}^2 = 0.077079\ kN$. The equation of the "forces method" for the rod in Figure 4b has the form:

$$\frac{18}{\lambda_1}\left(\frac{1}{\lambda_1} - \frac{1}{\tan \lambda_1}\right) + \frac{36 \tan \lambda_2}{\lambda_2(\tan \lambda_2 - \lambda_2)}\left(\tan \frac{\lambda_2}{2} - \frac{\lambda_2}{2}\right) = 0. \tag{31}$$

Solving equation (31), we obtain $\lambda_{1,cr} = 3.053638$, $P_{cr} = \frac{1}{2 \cdot 36} \lambda_{1,cr}{}^2 = 0.1295098\ kN$.

In Table 2, in addition to the exact values, the values of the critical load are given, which are determined using a finite element with 5 degrees of freedom and the results of calculations using the LIRA-SAPR program for the rods in Figure 4.

***Table 2. Critical forces for straight rods with an intermediate support (Figure 4)***

| Rod | Finite element with five degrees of freedom | | Finite element with three degrees of freedom, LIRA-SAPR | | Exact decision, $P_{cr},\ kN$ |
|---|---|---|---|---|---|
| | $P_{cr},\ kN$ | Error, % | $P_{cr},\ kN$ | Error, % | |
| Figure 4a | 0.077158 | 0.10 | 0.097055 | 25.9 | 0.0770790 |
| Figure 4b | 0.129967 | 0.35 | 0.175336 | 35.4 | 0.1295098 |

The obtained results confirm the high accuracy of determining the critical forces when using the finite element with five degrees of freedom. Since the proposed finite element quite accurately simulates the stress-strain state of compressed-bent rods with different types of supports, it can be confidently asserted that for arbitrary rod systems, this finite element will allow us to determine the values of the critical forces with sufficiently high accuracy.
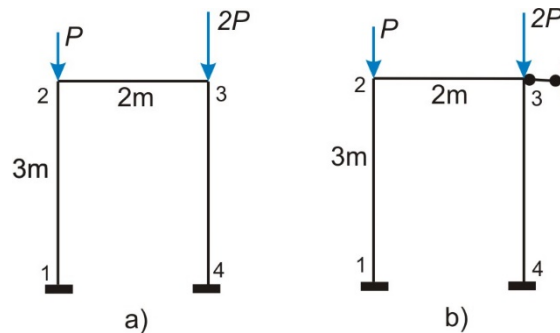


**Figure 5. Single-span frame with clamped ends**

Calculations have also been performed to determine the critical load for a single-span frame shown in Figure 5. The lengths of the rods are shown in the figure. The flexural rigidity of the rods is $EI = 10\ kH/m^2$, longitudinal stiffness $EA = 100\ kH$, $P = 10\ kH$. The critical load parameter was determined by using from 1 to 8 finite elements for modeling each rod (Table 3).

***Table 3. Critical loading parameter $\lambda_{cr}$ for frames (Figure 5)***

| Crushing of rods into finite elements | The frame in Figure 5a | | | The frame in Figure 5b | | |
|---|---|---|---|---|---|---|
| | Finite element with three degrees of freedom, LIRA-SAPR | Finite element with five degrees of freedom | Difference of the results, % | Finite element with three degrees of freedom, LIRA-SAPR | Finite element with five degrees of freedom | Difference of the results, % |
| 1 | 0.5171 | 0.51200 | 0.99 | 3.2898 | 1.66299 | 97.8 |
| 2 | 0.5135 | 0.51199 | 0.27 | 1.6711 | 1.63717 | 2.07 |
| 4 | 0.5121 | 0.51199 | 0.02 | 1.6421 | 1.63712 | 0.3 |
| 8 | 0.5120 | 0.51199 | 0.02 | 1.6375 | 1.63712 | 0.02 |

For the frame in Figure 5a, the critical load parameter, calculated using a finite element with five degrees of freedom in the node, practically does not change when the rods are crushed. If we use a classical finite element with three degrees of freedom, then $\lambda_{cr}$ with an increase in crushing of the rods to

8 finite elements decreases by approximately 1 % and becomes equal to the critical parameter calculated using a finite element with five degrees of freedom without crushing the rods.

For a frame with an additional support (Figure 5b), which excludes horizontal displacement, the change in the critical parameter during crushing of rods for finite elements with three degrees of freedom is more significant (Table 3). If you don't divide the rods into few finite elements, then the critical parameter is almost twice as large as the parameter obtained by using one element with five degrees of freedom. When dividing each rod into 2 finite elements, the difference of solutions is only 2 %. With further crushing of the rods, the results become practically equal.
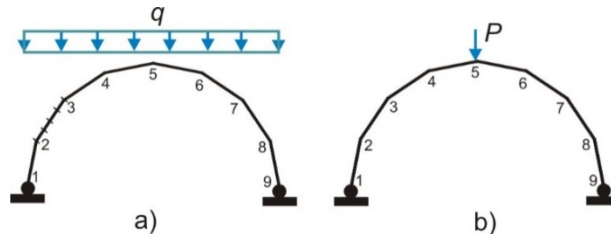


**Figure 6. Frame from eight rods inscribed in a circle, with hinged supports**

Figure 6 shows a frame, which inscribed in a circle of radius R = 6 *m*. The frame consists of eight straight rods. The flexural rigidity of the rods is $EI = 10 \ kH/m^2$, longitudinal stiffness $EA = 100 \ kH$. We considered loading in a form uniformly distributed load and in a form single concentrated force. The critical load parameter was determined for the additional dividing all the rods by 1, 2, 4, 8, and 16 finite elements (Table 4). In Fig. 6a shows an example of dividing the rod (2-3) into 4 finite elements.

*Table 4. Critical loading parameter $\lambda_{cr}$ for the frame (Figure 6)*

| Crushing of rods into finite elements | The frame in Figure 6a | | | The frame in Figure 6b | |
|---|---|---|---|---|---|
| | Finite element with three degrees of freedom, LIRA-SAPR | Finite element with five degrees of freedom | Difference of the results, % | Finite element with three degrees of freedom, LIRA-SAPR | Finite element with five degrees of freedom |
| 1 | 0.1109 | 0.12341 | 10.1 | 1.7212 | 1.7212 |
| 2 | 0.1164 | 0.12341 | 5.7 | 1.7212 | 1.7212 |
| 4 | 0.1197 | 0.12341 | 3.0 | 1.7212 | 1.7212 |
| 8 | 0.1215 | 0.12341 | 1.5 | 1.7212 | 1.7212 |
| 16 | 0.1224 | 0.12341 | 0.8 | 1.7212 | 1.7212 |

The results of calculations for the frame in Figure 6 show, that with additional crushing of the rods into finite elements (from 1 to 16):

1. for a finite element with five degrees of freedom – critical load parameter $\lambda_{cr}$ does not change for both loading schemes;

2. for a finite element with three degrees of freedom – value of the critical load parameter $\lambda_{cr}$, for the action of the distributed load (Figure 6a), increases by approximately 10 % and approaches the value obtained for a finite element with five degrees of freedom (Figure 7);

3. for a finite element with three degrees of freedom – value of the critical load parameter $\lambda_{cr}$, for the action of a concentrated load (Figure 6b), does not change and is equal to the value obtained for a finite element with five degrees of freedom.
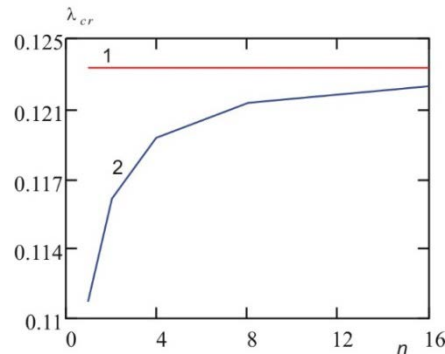
Тюкалов Ю.Я. Улучшенный стержневой конечный элемент для решения задач устойчивости // Инженерно-строительный журнал. 2018. № 3(79). С. 54–65.

**Figure 7. Changing the parameter $\lambda_{cr}$ for the frame in Figure 6a, depending
on the division of the rods into finite elements.
1– for finite element with 5 degrees of freedom; 2 – for finite element with 3 degrees of freedom.**

Figure 8 and Table 5 show the results of calculating the critical load parameter for a three-story frame, depending on the number of finite elements into which each rod of the frame is divided. The flexural rigidity of the rods is $EI = 10 \ kH/m^2$, longitudinal stiffness $EA = 100 \ kH$. The columns of the frame are rigidly clamped, and the crossbars have hinged fixed supports.
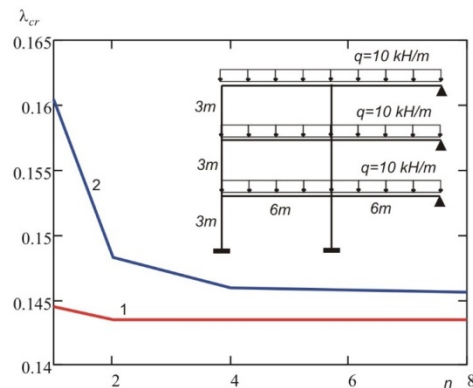


**Figure 8. Changing the parameter $\lambda_{cr}$ for the three-story frame, depending
on the division of the rods into finite elements.
1 – for finite element with 5 degrees of freedom; 2 – for finite element with 3 degrees of freedom.**

*Table 5. Critical loading parameter $\lambda_{cr}$ for the frame (Figure 8)*

| Crushing of rods into finite elements | Finite element with three degrees of freedom, LIRA-SAPR | Finite element with five degrees of freedom |
|---|---|---|
| 1 | 0.1605 | 0.1445 |
| 2 | 0.1482 | 0.1434 |
| 4 | 0.1459 | 0.1434 |
| 8 | 0.1456 | 0.1434 |

The results of calculations for the frame in Figure 8 show, that with additional crushing of the rods into finite elements (from 1 to 8):

1.  for finite elements with five degrees of freedom, the critical load parameter $\lambda_{cr}$ decreases by 0.8 %, when rods divided by two finite elements, and does not change with further crushing of the rods;

2.  for finite elements with three degrees of freedom, the value of the critical load parameter $\lambda_{cr}$ decreases by approximately 9 % and approaches the value obtained for finite element with five degrees of freedom.

## 4.   Conclusion

1.  The introduction of additional degrees of freedom at the nodes, in the form of the curvature of the axis and longitudinal deformation, makes it possible in many cases to more accurately determine the

magnitude of the critical load. In this case, the system has more degrees of freedom, so the approximation of the forms of stability loss is more accurate.

2. For some calculation schemes, for example, shown in Figures 3–5, when using a classical finite element with three degrees of freedom, the critical parameter is determined with a significant error of 20 % to 100 %. To increase the accuracy of determining the critical load, it is necessary to divide the rods into several finite elements. When using a finite element with five degrees of freedom, the error in calculating the critical parameter is no more than 10.1 % without additional crushing of the rods.

3. For computational schemes, in which there are no distributed loads and in which there are enough degrees of freedom in the form of displacements of nodes along the coordinate axes, the solutions for the two finite elements under consideration coincide.

4. For the frame in Figure 6, for finite element with three degrees of freedom, with additional division of the rods into finite elements, the value of the critical load parameter increases and approaches the value obtained for the finite element with five degrees of freedom.

5. For the frame in Figure 8, for finite element with three degrees of freedom, with additional division of the rods into finite elements, the value of the critical load parameter decreases by approximately 9 %, and approaches the value, obtained for the finite element with five degrees of freedom.

6. The use of the finite element with five degrees of freedom will avoid possible large errors in the determination of critical forces for design schemes in which no additional crushing of the rods into finite elements is used.

### References

1. Zenkevich O. *Metod konechnykh elementov v tekhnike* [Finite element method in engineering]. Moscow: Mir, 1975. 541 p.(rus)

2. Zenkevich O., Morgan K. *Konechnyye elementy i approksimatsiya* [Finite Elements and Approximation]. Moscow: Mir, 1986. 318 p.(rus)

3. Gallager R. *Metod konechnykh elementov. Osnovy* [Finite element method. Basics]. Moscow: Mir, 1984. 428 p.(rus)

4. Yevzerov I.D. Stability problems for rods and plates]. *Magazine of Civil Engineering.* 2014. No. 1(45). Pp. 6–11. (rus)

5. Noor A.K., Green W.H., Hartley S.J. Nonlinear finite element analysis of curved beams. *Comput. Meth. Appl. Mech. and Eng.* 1977. Vol. 12. No. 3. Pp. 289–307.

6. Schmidt W.F. Nonlinear bending of beams using the finite element method. *Comput. and Struct.* 1978. Vol. 8. No. 1. Pp. 153–158.

7. Tuna M., Kirca M. Exact solution of Eringen's nonlocal integral model for bending of Euler–Bernoulli and Timoshenko beams. *International Journal of Engineering Science.* 2016. Vol. 105. Pp. 80–92.

8. Kucukler M., Gardner L., Macorini L. Flexural–torsional buckling assessment of steel beam–columns through a stiffness reduction method. *Engineering Structures.* 2015. Vol. 101. Pp. 662–676.

9. Zhong H., Zhang R., Yu H. Buckling analysis of planar frameworks using the quadrature element method. *International Journal of Structural Stability and Dynamics.* 2011. Vol. 11. No. 2. Pp. 363–378.

10. Xiao N., Zhong H. Non-linear quadrature element analysis of plane frames based on geometrically exact beam theory. *Int. J. Non-linear Mech.* 2012. Vol. 47. Pp. 481–488.

11. Javidinejad A. Buckling of beams and columns under combined axial and horizontal loading with various axial loading application location. *Journal of Theoretical and Applied Mechanics.* 2012. Vol. 42. No. 4. Pp. 19–30.

12. Yuan W.B., Kim B., Li L. Y. Buckling of axially loaded castellated steel columns. *J. Construct. Steel Res.* 2014. No. 92. Pp. 40–45.

13. Soltani M.R., Bouchaïr A., Mimoune M. Nonlinear FE analysis of the ultimate behaviour of steel castellated

### Литература

1. Зенкевич О. Метод конечных элементов в технике. М.: Мир, 1975. 541 с.

2. Зенкевич О., Морган К. Конечные элементы и аппроксимация. М.: Мир, 1986. 318 с.

3. Галлагер Р. Метод конечных элементов. Основы. М.: Мир, 1984. 428 с.

4. Евзеров И.Д. Задачи устойчивости для стержней и пластин// Инженерно-строительный журнал. 2014. № 1(45). С. 6–11.

5. Noor A.K., Green W.H., Hartley S.J. Nonlinear finite element analysis of curved beams // Comput. Meth. Appl. Mech. and Eng. 1977. Vol. 12. № 3. Pp. 289–307.

6. Schmidt W.F. Nonlinear bending of beams using the finite element method // Comput. and Struct. 1978. Vol. 8. № 1. Pp. 153–158.

7. Tuna M., Kirca M. Exact solution of Eringen's nonlocal integral model for bending of Euler–Bernoulli and Timoshenko beams // International Journal of Engineering Science. 2016. Vol. 105. Pp. 80–92.

8. Kucukler M., Gardner L., Macorini L. Flexural–torsional buckling assessment of steel beam–columns through a stiffness reduction method // Engineering Structures. 2015. Vol. 101. Pp. 662–676.

9. Zhong H., Zhang R., Yu H. Buckling analysis of planar frameworks using the quadrature element method // International Journal of Structural Stability and Dynamics. 2011. Vol. 11. № 2. Pp. 363–378.

10. Xiao N., Zhong H. Non-linear quadrature element analysis of plane frames based on geometrically exact beam theory // Int. J. Non-linear Mech. 2012. Vol. 47. Pp. 481–488.

11. Javidinejad A. Buckling of beams and columns under combined axial and horizontal loading with various axial loading application location // Journal of Theoretical and Applied Mechanics. 2012. Vol. 42. № 4. Pp. 19–30.

12. Yuan W.B., Kim B., Li L.Y. Buckling of axially loaded castellated steel columns // J. Construct. Steel Res. 2014. № 92. Pp. 40–45.

13. Soltani M.R., Bouchaïr A., Mimoune M. Nonlinear FE analysis of the ultimate behaviour of steel castellated beams // J. Constr. Steel Res. 2012. Vol. 70. Pp. 101–114.

14. Salem A.H., El Dib F.F., El Aghoury M., Hanna M.T.

beams. *J. Constr. Steel Res.* 2012. Vol. 70. Pp. 101–114.

14. Salem A.H., El Dib F.F., El Aghoury M., Hanna M.T. Elastic stability of planar steel frames with unsymmetrical beam loading. *Journal of structural engineering.* 2004. Vol. 130. No. 11. Pp. 1852–1859.

15. Manuylov G.A., Kositsyn S.B., Begichev M.M. Chislennoye issledovaniye prostranstvennoy ustoychivosti uprugikh krugovykh zashchemlennykh arok [Numerical study of the spatial stability of elastic circular pinched arches]. *International Journal for Computational Civil and Structural Engineering.* 2013. Vol. 9. No. 1. Pp. 78–84.(rus)

16. Senjanović I., Vladimir N., Cho D.-S. A simplified geometric stiffness in stability analysis of thin-walled structures by the finite element method. *Inter J. Nav. Archit. Oc. Engng.* 2012. Vol. 4. Pp. 313–321.

17. Lalin V., Rybakov V., Alexander S. The finite elements for design of frame of thin-walled beams. *Applied Mechanics and Materials.* 2014. Vol. 578-579. Pp. 858–863.

18. Lalin V.V., Rozin L.A., Kushova D.A. Variatsionnaya postanovka ploskoy zadachi geometricheski nelineynogo deformirovaniya i ustoychivosti uprugikh sterzhney [Variational formulation of the plane problem of geometrically nonlinear deformation and stability of elastic rods]. *Magazine of Civil Engineering.* 2013. No. 1(36). Pp. 87–96.(rus)

19. Qiu W., Demkowicz L. Mixed hp-finite element method for linear elasticity with weakly imposed symmetry: stability analysis. *SIAM J. Numer. Anal.* 2011. Vol. 49. No. 2. Pp. 619–641.

20. Kim B., Li L., Edmonds A. Analytical solutions of lateral–torsional buckling of castellated beams. *International Journal of Structural Stability and Dynamics.* 2016. Vol. 16. No. 8. Pp. 443–455.

21. Blyumin S.L., Zverev V.V., Sotnikova I.V., Sysoyev A.S. Resheniye zadachi ustoychivosti szhato-izgibayemykh zhestko opertykh sterzhney peremennoy zhestkosti[The solution of the problem of the stability of squeezed-bent rigidly supported rods of variable rigidity]// Vestnik MGSU. 2015. No. 5. Pp. 18—26.(rus)

22. Dubrovin V.M., Butina T.A. Modelirovaniye ustoychivosti szhatogo i skruchennogo sterzhnya v tochnoy postanovke zadachi[Simulation of the stability of a compressed and twisted rod in the exact formulation of the problem]. *Matematicheskoye modelirovaniye i chislennyye metody.* 2015. No. 3. Pp. 3–16.(rus)

23. Kuo Y.-L. Stress-based finite element analysis of sliding beams. *Appl. Math. Inf. Sci.* 2015. Vol. 9. No. 2. Pp. 609–616.

24. Tyukalov Yu.Ya. The functional of additional energy for the analysis of the stability of spatial rod systems. *Magazine of Civil Engineering.* 2017. No. 2(70). Pp. 18–32. (rus)

25. Tyukalov Yu.Ya. *Raschet zhelezobetonnykh ploskikh sterzhnevykh sistem na kratkovremennyye dinamicheskiye vozdeystviya s uchetom fizicheskoy nelineynosti* [Calculation of reinforced concrete flat rod systems on short-term dynamic influences taking into account physical nonlinearity]. PhD dissertation. Kirov, 1990. 140 p.(rus)

26. Timoshenko S. P. Ustoychivost sterzhney, plastin i obolochek [Stability of rods, plates and shells]. Moscow: Nauka, 1971. 808 p.(rus)

Elastic stability of planar steel frames with unsymmetrical beam loading // Journal of structural engineering. 2004. Vol. 130. № 11. Pp. 1852–1859.

15. Мануйлов Г.А., Косицын С.Б., Бегичев М. М. Численное исследование пространственной устойчивости упругих круговых защемленных арок// International Journal for Computational Civil and Structural Engineering. 2013. Vol. 9. № 1. Pp. 78–84.

16. Senjanović I., Vladimir N., Cho D.-S. A simplified geometric stiffness in stability analysis of thin-walled structures by the finite element method // Inter J. Nav. Archit. Oc. Engng. 2012. Vol. 4. Pp. 313–321.

17. Lalin V., Rybakov V., Alexander S. The finite elements for design of frame of thin-walled beams// Applied Mechanics and Materials. 2014. Vol. 578–579. Pp. 858–863.

18. Лалин В.В., Розин Л.А., Кушова Д.А. Вариационная постановка плоской задачи геометрически нелинейного деформирования и устойчивости упругих стержней // Инженерно-строительный журнал. 2013. № 1(36). С. 87–96.

19. Qiu W., Demkowicz L. Mixed hp-finite element method for linear elasticity with weakly imposed symmetry: stability analysis // SIAM J. Numer. Anal. 2011. Vol. 49. № 2. Pp. 619–641.

20. Kim B., Li L., Edmonds A. Analytical solutions of lateral–torsional buckling of castellated beams // International Journal of Structural Stability and Dynamics. 2016. Vol. 16. № 8. Pp. 443–455.

21. Блюмин С.Л., Зверев В.В., Сотникова И.В., Сысоев А.С. Решение задачи устойчивости сжато-изгибаемых жестко опертых стержней переменной жесткости // Вестник МГСУ. 2015. № 5. С. 18–26.

22. Дубровин В.М., Бутина Т.А. Моделирование устойчивости сжатого и скрученного стержня в точной постановке задачи // Математическое моделирование и численные методы. 2015. № 3. С. 3–16.

23. Kuo Y.-L. Stress-based finite element analysis of sliding beams // Appl. Math. Inf. Sci. 2015. Vol. 9. № 2. Pp. 609–616.

24. Тюкалов Ю.Я. Функционал дополнительной энергии для анализа устойчивости пространственных стержневых систем // Инженерно-строительный журнал. 2017. № 2(70). С. 18–32.

25. Тюкалов Ю.Я. Расчет железобетонных плоских стержневых систем на кратковременные динамические воздействия с учетом физической нелинейности : диссертация ... кандидата технических наук : 05.23.17. - Киров, 1990. 140 с.

26. Тимошенко С.П. Устойчивость стержней, пластин и оболочек. М.: Наука, 1971. 808 с.

*Yury Tyukalov,*
*+7(912)8218977; yutvgu@mail.ru*

*Юрий Яковлевич Тюкалов,*
*+7(912)8218977; эл. почта: yutvgu@mail.ru*